Tellus (2001), 53B, 273–287
Printed in UK. All rights reserved

TELLUS
ISSN 0280–6509

Dimethylsulphide production in the subantarctic southern ocean under enhanced greenhouse conditions

By ALBERT J. GABRIC*[1], PETER H. WHETTON[2] and ROGER CROPP[1], [1]*School of Australian Environmental Studies, Griffith University, Nathan, 4111 Australia;* [2]*CSIRO Division of Atmospheric Research, Private Bag 1, Aspendale, 3195, Australia*

(Manuscript received 11 September 2000; in final form 10 January 2001)

ABSTRACT

Dimethylsulphide (DMS) is an important sulphur-containing trace gas produced by enzymatic cleavage of its precursor compound, dimethylsulphoniopropionate (DMSP), which is released by marine phytoplankton in the upper ocean. After ventilation to the atmosphere, DMS is oxidised to form sulphate aerosols which in the unpolluted marine atmosphere are a major source of cloud condensation nuclei (CCN). Because the micro-physical properties of clouds relevant to climate change are sensitive to CCN concentration in air, it has been postulated that marine sulphur emissions may play a rôle in climate regulation. The Subantarctic Southern Ocean (41–53°S) is relatively free of anthropogenic sulphur emissions, thus sulphate aerosols will be mainly derived from the biogenic source of DMS, making it an ideal region in which to evaluate the DMS-climate regulation hypothesis. We have extended a previous modelling analysis of the DMS cycle in this region by employing a coupled general circulation model (CGCM) which has been run in transient mode to provide a more realistic climate scenario. The CGCM output provided meteorological data under the IPCC/IS92a radiative forcing scenario. A DMS production model has been forced with the CGCM climate data to simulate the trend in the sea-to-air DMS flux for the period 1960 to 2080, corresponding to equivalent CO_2 tripling relative to pre-industrial levels. The results confirm a minor but non-negligible increase in DMS flux in this region, in the range +1% to +6% predicted over the period simulated. Uncertainty analysis of the DMS model predictions have confirmed the positive sign for the change in DMS flux, that is a negative DMS feedback on warming.

1. Introduction

Dimethylsulphoniopropionate (DMSP) is an organic sulphur compound produced by marine phytoplankton, although only certain species are significant producers (Keller et al., 1989). DMSP is enzymatically cleaved to dimethylsulphide (DMS), which is released to oceanic surface waters in concentrations which are high enough to sustain a net flux to the atmosphere, currently estimated to be 0.5 ± 0.3 Tmol S yr^{-1} (Erikson et al., 1990; Bates et al., 1992). DMS concentration in the upper ocean seems to be primarily controlled by biological cycling in the marine pelagic food web (Kiene and Bates, 1990; Leck et al., 1990; Levasseur et al., 1996), although photo-oxidation can also be an important sink in some regions (Kieber et al., 1996).

Once ventilated to the atmosphere, DMS is oxidised to form non-sea-salt sulphate (nss-SO_4^{2-} and methanesulphonate (MSA) aerosols. It has been suggested that the major source of cloud condensation nuclei (CCN) in unpolluted marine atmospheres such as the Southern Ocean is the biogenic production of. DMS (Ayers and Gras,

* Corresponding author.
e-mail: a.gabric@mailbox.gu.edu.au

1991). Because the micro-physical properties of clouds are sensitive to CCN concentration in the atmosphere, it has been postulated (Charlson et al., 1987; Meszaros, 1988; Shaw, 1983) that biological regulation of the Earth's radiation budget is possible through a DMS-CCN-cloud albedo link. Both Foley et al. (1991) and Lawrence (1993) have shown that the magnitude of climate feedback associated with the DMS cycle could be significant. Although regional analyses (Gabric et al., 1998) suggest that the DMS-climate feedback is indeed negative, there is still considerable uncertainty as to the magnitude and sign of the global feedback (Liss et al., 1994).

The sea-to-air flux of DMS depends on the concentration of DMS in the upper ocean and the magnitude of the DMS sea-to-air transfer velocity. The sea-water concentration of DMS depends in a complex way on both the planktonic food-web structure, and external forcings such as sea temperature and irradiance. The transfer velocity has been parameterised as function of sea surface temperature and wind speed, but is also thought to depend on wind-waves and the presence of surfactants (Jahne and Haussecker, 1998).

Here we investigate the effect of simulated climate change on the sea-to-air flux of DMS in a study region in the Subantarctic Southern Ocean. We have chosen the Subantarctic Southern Ocean for this numerical experiment as it is relatively unaffected by anthropogenic sources and thus the production of sulphate aerosols will be mainly due to the biogenic source of DMS. Furthermore, analysis of a long time series of atmospheric measurements at Cape Grim, Tasmania (40°41′S, 144°41′E) has confirmed the connection between atmospheric DMS and aerosol sulphur species in this region (Ayers et al., 1991; Boers et al., 1994).

Although there is little data on dissolved DMS concentration in the Southern Ocean (Kettle et al., 1999), excellent agreement between the oceanic and atmospheric model estimates of the DMS flux has been obtained for the study region (Gabric et al., 1995). Recently, a "slab-ocean" (constant mixed layer depth) general circulation model (GCM) was used to provide meteorological forcings under two climate scenarios: present CO_2 concentration and an instantaneous doubling of CO_2 (Gabric et al., 1998, hereafter G98) relative to pre-industrial levels. The GCM simulation under doubled CO_2 conditions predicted a warming of around 4°C for our study region, together with a small decrease (3%-5%) in monthly mean wind speeds throughout the year. The impact on the annual integrated DMS flux (an increase in the range 2% to 8%) provided evidence that the sign of the DMS-climate feedback is indeed negative, as hypothesised by Charlson et al. (1987), but relatively small.

The present study seeks to better quantify the size of the feedback. As opposed to a slab ocean model used in G98, here we employ a full ocean–atmosphere GCM which has been run in transient mode. This provides a detailed representation of the changes in the upper ocean in our study region under enhanced green-house conditions. To gauge the impact on biogenic sulphate emissions, the DMS production model has been run using the GCM predicted forcings for the period 1961–2080, up to the time of approximate CO_2 tripling relative to pre-industrial levels.

2. Characteristics of study area

The study region was defined as the area of the ocean where in situ DMS production may affect atmospheric DMS concentrations measured at the Cape Grim station, where sampling is carried out during baseline conditions–periods during which the 10 m wind direction is from the southwest quadrant (190°–280°). The extent of the study region upwind of the Cape Grim baseline is determined by the mean wind speeds, and the lifetime of gaseous DMS in the marine boundary layer. As monthly mean wind speeds at Cape Grim range between 11 m s^{-1} in January to 7 m s^{-1} in June, an air parcel can travel up to 1000 km per day (Wilson and Ayers, 1990). Since the lifetime of gaseous DMS varies from approximately half a day in summer to about a week in winter (Koga and Tanaka, 1993), the atmospheric DMS concentrations observed at Cape Grim may be influenced by oceanic production in a quadrant over 2000 km upwind of Cape Grim as shown in Fig. 1.

Analysis of archival satellite imagery of the Southern Ocean between 38–51°S (Gabric et al., 1996) showed that a well-defined spring bloom event is not typical of these waters; however, phytoplankton biomass is enhanced in the spring-summer period and depressed during winter. This is confirmed by field data (Clementson et al., 1998)

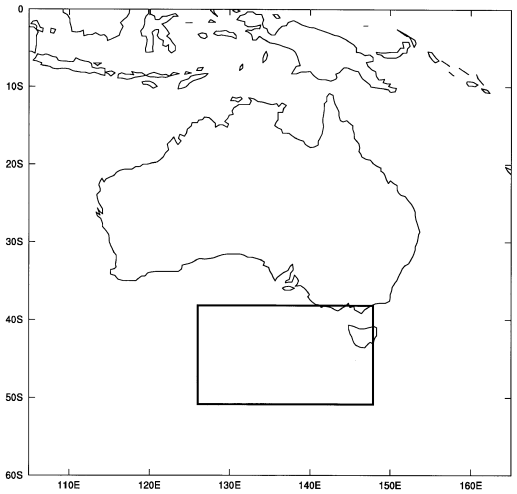

Fig. 1. The Southern Ocean study region used for the model simulations.

that report mixed-layer nitrate levels are typically very high in late winter and early spring.

The field measurements of dissolved DMS made in the study region between 1991–1995 have been summarised by Curran et al. (1998). Maximum DMS concentrations in the Subantarctic zone were high (range: not detectable — 6 nM) but variable in spring and summer. McTaggart and Burton (1992) recorded mean January DMS surface concentrations of 20.5 nM, in the study area during the 1988–89 austral summer, a high value compared to the global mean concentration of 5.3 nM (Kettle et al., 1999). Jones et al. (1998) recorded lower DMS levels along a north–south transect during ACE-1 (First Aerosol Characterisation Experiment) during November–December 1995, with values in the range not detectable — 5.6 nM. However, high nitrate levels (mean $>10\,\mu M$) and low chlorophyll readings (0.04–0.6 $\mu g\ L^{-1}$) suggest that during the ACE-1 experiment, biological activity was still depressed, and that the peak algal growth period may have come later in the summer.

As DMS concentrations are affected by the phytoplankton community's taxonomy, it is important to have data on the species present in the study region. Jones et al. (1998) reported that the phytoplankton community during late spring was dominated by diatoms (*Thalassiosira* and *Tropidoneis*) and dinoflagellates (*Gymnodinium, Exuviaella* and *Protoperidinium*). The earlier study of McTaggart and Burton (1992) reported that coccolithophores were common north of the Antarctic Convergence (53°S) during January. A summary of the DMS and oceanographic field data for the study region is given in Table 1.

3. Methods

3.1. The general circulation model

The transient climate data were obtained from simulations with the Commonwealth Scientific and Industrial Research Organisation (CSIRO) coupled climate model (Gordon and O'Farrell, 1997) which includes ocean, atmosphere and sea-ice components. The horizontal resolution of the atmospheric model is 5.6° of longitude by 3.2° of latitude (strictly it is a spectral model of R21 resolution) and it has nine vertical levels. The sea-ice model was described in O'Farrell (1997). The ocean model is based on the Bryan–Cox code (Cox, 1984) with 21 vertical levels. Previous experiments with coupled ocean–atmosphere models yielded unrealistically large (1–2 km) late winter mixing in the sub-polar Southern Ocean. This deficiency has been partly remedied by use of the Gent and McWilliams (1990) scheme for parameterising the effect of sub-grid scale mixing. Further details of the ocean component are given

Table 1. *Summary of field data in the study region (nd: not detectable)*

Ref.	Nitrate (μM)	DMS (nM)	Chl-a (mg m^{-3})	MLD (m)	Ze (m)	DOY
Curran et al. (1998)		nd–6.0				spring/summer
De Bruyn et al. (1998)		0.4–6.8				spring/summer
Griffiths et| al. (1999)	10–30		0.2–1.2	8–61	60–78	322–340
Jones et al. (1998)	3–28	nd–5.6	0.04–0.66	8–89	60–75	321–342
McTaggart and Burton (1992)		0.8–28				1–30

in Gordon and O'Farrell (1997) and Hirst et al. (2000).

The coupled GCM was initialised using the final spin-up state of the atmosphere–ocean system which resulted from several thousand years of integration. The control integration used a constant equivalent CO_2 concentration of 330 ppm. The transient integration is subject to changing equivalent CO_2 concentration as specified in the IPCC/ISP92a radiative forcing scenario following the prescription of Kattenberg et al. (1996) for the period from 1880 to 2080 (for details, see Hirst et al. (2000)).

A subset of the output from GCM simulations for the period 1961–2080 were obtained for the study area indicated in Fig. 1, which includes 16 (4×4) GCM horizontal grid points. The GCM simulation results were spatially averaged over the 16 grid-points and also temporally averaged to derive monthly means of surface wind speed, surface sea temperature, mixed layer depth and cloud cover. Although light limitation of phytoplankton growth is included in the DMS production model (see eq. (6) below), the GCM-simulated radiation data could not be used because shortwave radiation was not computed in the relevant band for phytoplankton growth, namely, the photosynthetically active range (PAR).

3.2. DMS marine production model

The DMS production model has been described previously in Gabric et al. (1993) and calibrated for the study area by comparison with atmospheric data on DMS collected at Cape Grim (Gabric et al., 1995, 1996). The model is time-dependent with state variables vertically averaged over the oceanic mixed layer. The mixed layer can vary throughout the year as prescribed by the output from the GCM simulation. Model equations are given in Tables 2 and 3, with parameter values or ranges given in Table 4. In order to conserve mass in the multi-annual simulations, settling of particulate matter below the thermocline (parameters k7, k22) is turned off.

The model food web includes 5 biotic variables: a generic autotroph (phytoplankton), heterotrophic bacteria, and three grazers, flagellates (bacterivores), large protozoa and zooplankton. In our previous work (Gabric et al., 1998) and in the present analysis it was assumed that climate change does not significantly modify the structure of the marine food web in this region.

In the following discussion, we focus on those parts of the DMS model formulation that are sensitive to changes in either sea-surface temperature (SST), wind speed (w), cloud cover (CC) or mixed layer depth (MLD). From a climate feedback perspective, the important variable is the sea-to-air flux of DMS, given by the product of the sea-to-air DMS transfer velocity and the change in concentration in DMS across the sea-air interface. Since the sea-water DMS concentration, $[\mathrm{DMS}]_{\mathrm{aq}}$, is typically much greater than the atmospheric concentration (Berresheim et al., 1991), this flux may be approximated by,

$$F_{\mathrm{DMS}} = k_{\mathrm{w}}\,[\mathrm{DMS}]_{\mathrm{aq}}. \tag{1}$$

The transfer velocity k_{w} has been parameterised in terms of wind speed, w, and ocean temperature according to the formulation of Liss and Merlivat (1986) as adapted for DMS by Gabric et al. (1995),

$$k_{\mathrm{w}} = \alpha 0.17w \qquad \text{for } w \leqslant 3.6 \tag{2a}$$

Table 2. *DMS model equations given in terms of fluxes defined in Table 3*

State variable (units)	Model equation
P: generic autotroph (mg N m^{-2})	$(dP/dt) = f_{61} - f_{12} - f_{14} - f_{15} - f_{1w}$
B: planktonic bacteria (mg N m^{-2})	$(dP/dt) = f_{12} + f_{62} - f_{23} - f_{26}$
F: bacterivorous nanoflagellates (mg N m^{-2})	$(dP/dt) = f_{23} - f_{36} - f_{34}$
LP: large protozoa (mg N m^{-2})	$(dLP/dt) = f_{34} + f_{14} - f_{45} - f_{46}$
Z: micro/mesozooplankton (mg N m^{-2})	$(dZ/dt) = f_{45} + f_{15} - f_{56} - f_{5w}$
N: dissolved inorganic nitrogen (mg N m^{-2})	$(dN/dt) = f_{26} + f_{36} + f_{46} + f_{56} - f_{61} - f_{62}$
DMSP: dissolved DMSP (mg S(DMSP) m^{-2})	$(dDMSP/dt) = f_{17} + f_{47} + f_{57} - f_{78} - f_{72}$
DMS: dissolved DMS (mg S(DMS) m^{-2})	$(dDMS/dt) = f_{18} + f_{78} - f_{82} - f_{8w} - f_{8a}$

Table 3. *Model flux definitions*

Flux	Formulation	Description
f_{12}	$k_1 * B * P/[P + k_2]$	bacterial decomposition of detrital phytoplankton (P)
f_{14}	$k_3 * P * LP$	grazing of P by large protozoa (LP)
f_{15}	$k_4 * P * Z$	grazing of P by zooplankton (Z)
f_{17}	$k_5 * \gamma * P$	release of DMSP by P
f_{18}	$\gamma * k_6 * P$	release of DMS by P, g is the DMSP
f_{1w}	$k_7 * P$	respiration and sedimentation of P below thermocline
f_{23}	$k_8 * F * B/[B + k_9]$	grazing on bacteria (B) by zooflagellates (F)
f_{26}	$k_{10} * B + k_{11} * [f_{62} + f_{12}]$	regeneration of dissolved nitrogen by B
f_{34}	$k_3 * F * \mathrm{LP}$	grazing on F by LP
f_{36}	$k_{13} * F + k_{14} * f_{23}$	regeneration of dissolved N by F
f_{45}	$k_{15} * \mathrm{LP} * Z$	grazing on LP by Z
f_{46}	$k_{16} * \mathrm{LP} + k_{17} * [f_{34} + f_{14}]$	excretion of dissolved N by LP
f_{47}	$\gamma * k_{18} * \mathrm{LP}$	excretion of DMSP by LP
f_{56}	$k_{19} * Z + k_{20} * [f_{15} + f_{45}]$	excretion of dissolved N by Z
f_{57}	$\gamma * k_{21} * Z$	excretion of DMSP by Z
f_{5w}	$k_{22} * f_{56} + k_{32} * Z$	sedimentation and export of Z
f_{61}	$R_L * R_T * k_{23} * P * N/[N + k_{24}]$	uptake of dissolved N by P (see eqns 4–5)
f_{62}	$k_{25} * B * N/[N + k_{26}]$	uptake of dissolved N by B
f_{72}	$k_{31} * \mathrm{DMSP}$	biodegradation of DMSP by B
f_{78}	$k_{27} * \mathrm{DMSP}$	conversion of DMSP to DMS in water column
f_{82}	$k_{28} * \mathrm{DMS}$	biodegradation of DMS by B
f_{8w}	$k_{29} * \mathrm{DMS}$	photo-oxidation sink for DMS
f_{8a}	$k_w * \mathrm{DMS}$	ventilation of DMS to atmosphere

$$k_w = \beta(2.85w - 10.3) + 0.61\alpha \qquad \text{for } 36 < w \leqslant 13 \tag{2b}$$

$$k_w = \beta(5.9w - 49.9) + 0.61\alpha \qquad \text{for } w > 13, \tag{2c}$$

with $\alpha = (600/\mathrm{Sc})^{2/3}$ and $\beta = (600/\mathrm{Sc})^{1/2}$. For a given gas, the Schmidt number (Sc) varies with water temperature, decreasing as the temperature increases. The dependence of Sc on sea surface temperature (SST) for DMS was experimentally derived by Saltzman et al. (1993) as,

$$\mathrm{Sc} = 2674.0 - 147.12\,(\mathrm{SST}) + 3.726\,(\mathrm{SST})^2 - 0.038\,(\mathrm{SST})^3. \tag{3}$$

As the GCM output did not include irradiance in the photosynthetic range, a radiation model based on that of Brock (1981) was used to compute the seasonal change in potential global irradiance, I_o (at top of the atmosphere). The irradiance at the sea surface I_s, is a function of cloud cover (CC), provided by the GCM, and is given by the following empirical relationship (Brutsaert, 1982; Pochop et al., 1968),

$$I_s = [a + b*(1 - 0.9*\mathrm{CC})/1.1]*I_o, \tag{4}$$

where the constants a and b depend on location and season. We have used the average values of ($a = 0.25$, $b = 0.5$) given by Brutsaert (1982). PAR at the sea-surface was estimated using the relation in Baker and Frouin (1987).

Phytoplankton growth is assumed to be affected by nutrient availability, light and temperature — the so-called multiplicative growth model (Platt et al., 1977). The specific nutrient uptake rate, μ, is thus given by,

$$\mu(t) = V_N(t)R_L(t)R_T(t), \tag{5}$$

where V_N (h^{-1}) is the nitrogen-specific nutrient uptake rate following standard Michaelis-Menten kinetics, and R_L and R_T are dimensionless light and temperature limitation coefficients (both $\leqslant 1$), respectively. The full form of eq. (5) is given in Table 2.

Light limitation of phytoplankton growth rate may be modelled using a number of formulations (Steele, 1962; Platt et al., 1980). Here we have chosen the relationship given by Smith (1936) as it involves a single parameter,

$$R_L = \frac{P}{P_{max}} = \left(\frac{I}{I_k}\right) \Big/ \sqrt{1 + \left(\frac{I}{I_k}\right)^2}, \tag{6}$$

Table 4. *Model parameter values (spatially dependent values are for 100 m MLD)*

Parameter	Value	Definition
k_1	4.5	max. uptake rate of detrital N by B (d^{-1})
k_2	4.6e-4	half-saturation conc. for B uptake of detrital N (mg N m^{-2})
k_3	2.6e-3	LP grazing rate per organism (m^2 mg N^{-1} d^{-1})
k_4	1.2e-4	Z grazing rate per organism (m^2 mg N^{-1} d^{-1})
k_5	0.01	release rate of DMSP by P (d^{-1})
k_6	0.85e-2	release rate of DMS by P (d^{-1})
k_7	0.0	P cell sinking rate (d^{-1})
k_8	17.0	max. uptake rate of B by F (d^{-1})
k_9	1.4e-3	half-saturation conc of B by F (mg N m^{-2})
k_{10}	0.07	B specific excretion rate (d^{-1})
k_{11}	0.63	proportion of N uptake excreted by B
k_{12}	1.6e-2	grazing rate of F by LP per organism (m^2 mg N^{-1} d^{-1})
k_{13}	0.05	F specific excretion rate (d^{-1})
k_{14}	0.65	proportion of N uptake excreted by F
k_{15}	1.2e-3	grazing rate of LP by Z per organism (m^2 mg N^{-1} d^{-1})
k_{16}	0.05	LP specific N excretion rate (d^{-1})
k_{17}	0.65	proportion of N uptake excreted by LP
k_{18}	0.01	DMSP excretion rate by LP (d^{-1})
k_{19}	0.10	Z specific N excretion rate (d^{-1})
k_{20}	0.4	proportion of N uptake excreted by Z
k_{21}	0.01	DMSP excretion rate by Z (d^{-1})
k_{22}	0.0	Z sinking rate (d^{-1})
k_{23}	0.9	max. N uptake rate by P (d^{-1})
k_{24}	1386.3	half-saturation conc. for N uptake by P (mg N m^{-2})
k_{25}	0.9	max. N uptake rate by B (d^{-1})
k_{26}	75.0	half-saturation conc. for N uptake by B (mg N m^{-2})
k_{27}	0.5	DMSP-DMS conversion rate (d^{-1})
k_{28}	0.95	DMS consumption rate by B (d^{-1})
k_{29}	1.3	maximum DMS photo-oxidation rate (d^{-1})
k_{31}	1.0	DMSP consumption rate by B (d^{-1})
k_{32}	0.0	Z export rate (d^{-1})
γ	0.3	mean algal cell S:N ratio (derived from algal cell DMSP content)
I_k	30–40	saturating irradiance (W m^{-2})

where P is the gross photosynthetic rate, P_{max} the maximum photosynthetic rate, I the irradiance at a particular depth, and I_k the saturating irradiance as defined by Talling (1957), which is species dependent (Raven and Richardson, 1986). During spring the phytoplankton community consist of a mix of diatoms and dinoflagellates, and I_k is likely to be in the range (20–40) W m^{-2} (Gabric et al., 1996).

The extent of the euphotic zone depends on surface irradiance and water column extinction which is affected by primary production. In these waters, the euphotic zone depth (Z_e), defined as the 1% illumination level, does not display much seasonal variability. The average light limitation may be computed by integrating R_L over the mixed layer depth; however, a very good approximation is obtained by substituting the mixed layer averaged irradiance for I in (6). The average irradiance I_{av} over the mixed layer depth, Z_m, is given by,

$$I_{av} = \frac{I_s}{kZ_m}[1 - e^{-kZ_m}], \tag{7}$$

where k is the light extinction coefficient, which may be derived from measurements of Z_e.

Laboratory culture studies show a clear temperature effect on the growth rate of phytoplankton (Eppley, 1972; Goldman and Carpenter, 1974), with the maximum rate of growth roughly doubling for every 10°C increase in sea temperature. The dependence on temperature is given by,

$$R_T = e^{0.063(T - T_{max})}, \tag{8}$$

where T is the mixed layer temperature in degrees Celsius, and T_{max} the temperature at which maximum growth rate is achieved. The temperature at which optimal growth rate occurs is species dependent; however, as noted by Valiela (1995), there is often a poor correlation between ambient sea temperature and a species' physiological temperature response. We have assumed the phytoplankton community gradually adapts to the higher temperatures under warmed conditions, and we ignore any significant species shifts which might occur in the study region.

DMS and its biogenic precursor DMSP are both phytoplankton metabolites. DMSP occurs both in particulate and dissolved forms and can be biodegraded by cleavage into DMS and acrylate (Kiene, 1990; Stefels and Van Boekel, 1993) or

by demethylation to 3-methylmercaptopropionate (MMPA). Demethylation of MMPA produces 3-mercaptopropionate (MPA) which is catabolized with the elimination of H_2S to leave acrylate. Demethylations of DMSP to MMPA and thence to MPA are microbially mediated reactions (Taylor and Gilchrist, 1996). Methylotrophic bacteria also consume both DMS and DMSP in surface waters (Kiene and Bates, 1990; Wolfe and Kiene, 1993). Indeed, Kiene et al. (2000) recently reported that DMSP may be a significant source of both carbon and sulphur for bacteria in surface waters.

The model formulation assumes that DMS and DMSP production and consumption follow first-order kinetics. Modelled sinks for DMS include photochemical oxidation, microbial consumption and ventilation to the atmosphere. DMS photo-oxidation, which is a maximum at the surface, is scaled by the ratio of surface to average mixed layer irradiance. Photo-oxidation consequently varies diurnally and seasonally with changes in incident solar radiation and the MLD. Bacterial DMS and DMSP consumption rates were estimated from the literature (Kiene and Bates, 1990). The DMS and DMSP excretion rates by grazers were conservatively kept at the values used in Gabric et al. (1993), although significantly higher rates have been reported in laboratory grazing experiments (Wolfe et al., 1994).

The DMS model was forced using the GCM simulated time series of sea-surface temperature, wind speed, cloud cover and mixed layer depth over the period 1961–2080. In order to obtain a baseline for comparison, the DMS model was also run using the forcings as simulated in a 120-year GCM control integration (constant CO_2 concentration).

The DMS model was initialised with nutrient and biota concentrations which are typical of conditions in the study region in early spring. The timing of the onset of the spring bloom can exhibit large interannual variability in the study region (Harris et al., 1987). Since a precise initialisation of the model was not possible, the model was "spun up" by integrating for several decades using the GCM predicted forcings for the first year of the time series, until a repeating annual cycle was achieved. The DMS model was then run with the transient GCM forcings for the next 120 years. It should be noted that the DMS model was not run to equilibrium in the transient simulation.

The impact on the DMS flux cycle was evaluated by examining the trend in annual flux over the entire 120-year time period. The slope of the DMS flux trend line was derived by linear regression analysis.

As the model parameters are subject to measurement error, and may in some cases vary during the annual cycle, it is important to quantify the uncertainty in the predicted flux trend. This was estimated by a Monte-Carlo uncertainty analysis (UA) in which the 120-year transient simulations were repeated for different combinations of the most sensitive parameters given in Table 5 (except wind speed, which is prescribed by the GCM). The number of UA model runs was not prescribed beforehand, but continued until the distribution of trend line slope and intercept no longer changed significantly — approximately 400 individual model runs. Parameter set combinations for the UA were derived by randomly sampling each parameter from an assumed normal distribution with the mean value given in Table 3 and a standard deviation of 20% of the mean. A 20% error was deemed appropriate considering both analytical errors in measurement (generally less than 5%) and possible temporal variation of the parameter.

In an additional evaluation, the DMS model was run to pseudo-equilibrium using the GCM simulated forcings averaged over three decadal periods· current conditions (1991–2000), and (2028–37) and (2071–80), the periods of equivalent CO_2 doubling and tripling relative to pre-industrial levels. This was done to gauge whether the lack of precise initialisation of the model had any significant effect in the transient model runs.

Satellite data from the recently launched Sea-Viewing Wide Field-of-View (SeaWifs) sensor (Lewis, 1995) was collected for the study region for the period 1997–1999. This consisted of monthly mean chlorophyll concentration data, which was used to compare with the model predictions of phytoplankton biomass using averaged forcings for the 1991–2000 period. Conversion from nitrogen to chlorophyll units was made assuming a Redfield C:N ratio of 5.7 (by weight) and a typical carbon : chlorophyll ratio of 50 (Geider, 1987; Sarmiento et al., 1993).

The satellite sensor's optical penetration depth

is approximately 25–30% of the euphotic zone depth in oceanic waters (Smith, 1981), thus the satellite is effectively registering near surface chlorophyll concentration. Consequently, subsurface chlorophyll maxima may not be detected, and the satellite may underestimate the true euphotic zone chlorophyll-*a* concentration. To account for this source of error, an empirical relation derived by Morel and Berthon (1989), based on 3400 chlorophyll profile measurements in various oceanic regions, was used to estimate the total euphotic zone chlorophyll *a* from the satellite registered value. This value was scaled by the mean euphotic zone depth measured during ACE-1 (67 m) to give a euphotic zone average value.

4. Results and discussion

4.1. The GCM simulations

In order to better interpret the DMS model predictions, the GCM forcings data were statistically analysed for detectable trends over the 120-year period. The GCM output consisted of monthly mean values from January 1961 to December 2080 of the SST, cloud cover, surface wind speed and MLD. The data sets were first stratified seasonally, and summer, autumn, winter and spring three-month averages were calculated for each year of the time series. Linear trend analysis was then performed on the stratified data to detect any significant trends in these variables and the results presented in Table 6.

Table 5. *Most influential DMS model parameters/inputs (Camponlongo and Gabric, 1996)*

Parameter	Explanation	Rank
w	wind speed	1
k_4	phytoplankton–zooplankton grazing rate	2
k_{21}	zooplankton-DMSP release rate	3
k_{27}	DMSP-DMS conversion rate	4
γ	DMSP cell content	5
k_{28}	microbial consumption rate of DMS	6
k_{31}	microbial consumption rate of DMSP	7
k_{29}	DMS photo-oxidation rate	8
I_k	saturating light intensity for photosynthesis	9
DIN	initial nitrate concentration	10

The linear model consistently explains over 89% of the variation in the surface temperature. With a coefficient of variation (c.v.) of less than 8.5% for all seasons, precision is indicated. In contrast, the trend analysis produced reveals no significant results regarding projected cloud cover. Only in winter is more than 1% of the inter-annual variability explained. The high c.v. also indicates a lack of precision. Similarly, the results for wind speed over the period modelled do not prove to be significant. A maximum of less than 2.5% of the variation was explained. The results for the MLD indicate a linear trend is significant for all seasons, but varying degrees of the variability are explained. Less than 6% of the variance is explained in summer and autumn. The relative variability is extremely high.

In order to better compare the trends in the main forcing variables, the ten-year average annual cycle in SST and MLD has been plotted in Fig. 2a, b at the beginning of the time series and around the times for equivalent CO_2 doubling (2033) and tripling (2080) relative to pre-industrial levels. The GCM simulates a temperature increase of approximately 0.7°K for the period of doubled CO_2 and 2°K for the period of tripled CO_2. These changes are uniform throughout the annual cycle. Interestingly, the warming predicted for the study region under CO_2 doubling in the slab ocean GCM (Gabric et al., 1998) was much higher at 4°K. These comparative results are typical of those from other "slab-ocean" and "deep-ocean" models for the Southern Ocean (Whetton et al., 1996).

The GCM simulates a strong shoaling of the

Table 6. *Results of statistical analyses of GCM output stratified by season (values are r^2 and cv)*

GCM variable	Season			
	Summer	Autumn	Winter	Spring
surface temperature	0.93	0.89	0.94	0.95
	0.068	0.083	0.062	0.053
cloud cover	0.0055	0.0002	0.017	0.0037
	6.03	4.28	3.41	4.59
wind speed	0.024	0.0082	0.013	0.0077
	5.16	4.53	4.35	4.79
mixed layer depth	0.062	0.052	0.19	0.38
	28.63	26.31	15.8	7.86

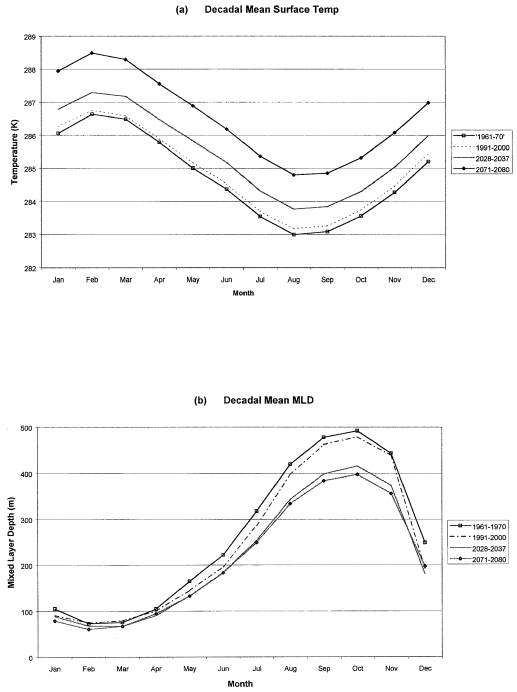

Fig. 2. Averaged annual cycle in GCM simulated forcing for 1961–70, 2029–38 and 2071–80 (a) surface temperature, (b) mixed layer depth.

MLD during the austral winter-spring for equivalent CO_2 doubling (2033), however, this trend is reduced by 2080. The mixed layer during spring is still quite deep ($\sim$400 m), and this change is unlikely to impact greatly on primary production or DMS emissions. Interestingly, the GCM predicts little change in the MLD during the austral summer. These findings support the recent speculations by Simo and Pedros-Alio (1999) regarding possible impacts of global warming on the MLD; however, our results suggest the timing of the MLD shoaling during the annual cycle may be critical to any impacts on DMS production.

4.2. *The DMS production cycle and annual cumulative flux*

The annual cycle in phytoplankton biomass derived from the satellite data for the 3-year period 1997–2000 is shown in Fig. 3. Only slight seasonal variability is evident in the mean euphotic zone chlorophyll-*a* value (range 0.28–0.34 mg m^{-3}); however, the variance in any month is high. Indeed, the satellite data suggests localised bloom events can occur in any month of the year. The mean mixed-layer chlorophyll-*a* reported during ACE-I (Nov.–Dec. 1995) was 0.38 mg m^{-3}, which compared well with the satellite-derived euphotic zone average values. However, it should be noted that the ACE-I data (Griffiths et al., 1999) reported deep chlorophyll maxima (near the bottom of the euphotic zone) were common in the study region, suggesting the possibility that the satellite values underestimate the true phytoplankton standing stock.

4.2.1. Transient runs. The predicted average annual cycles in phytoplankton and DMS mixed layer concentrations for current conditions (1991–2000) are shown in Fig. 4a. The model suggests that biomass will be higher in the spring-summer months, and damped in winter, but still at a moderate level. DMS concentrations also peak in spring–summer with the range in values consistent with field data (Table 1). A peak in phytoplankton is followed by a decline due to grazing by herbivores in the food-web. The cycle in DMS and biomass are slightly out of phase, with about 3–4 days between a peak in biomass and a subsequent peak in aqueous DMS concentration. This time lag is due to the continued release of DMSP and DMS by higher trophic components of the food web after the peak in phytoplankton biomass has passed (for discussion see Gabric et al., 1993).

The predicted DMS flux cycle is given in Fig. 4b, together with flux estimates made from atmospheric DMS data collected at Cape Grim by Ayers et al. (1995) and later corrected due to an underestimation of DMS removal rates in the earlier work (Ayers et al., 1996; Ayers, personal communication). The model and atmospheric flux estimates agree well during winter, spring and early summer, although the model seems to underestimate the late summer flux. This may be due to the model's inability to simulate a phytoplankton species succession, which may occur during late summer.

The predicted 120-year change in annual DMS flux (ΔF_{DMS}) for baseline model parameters is shown in Fig. 5. The high inter-annual variability reflects the variability in the GCM derived forcing data. A positive slope of the trend line corresponds to an increase in flux over the 120-year period.

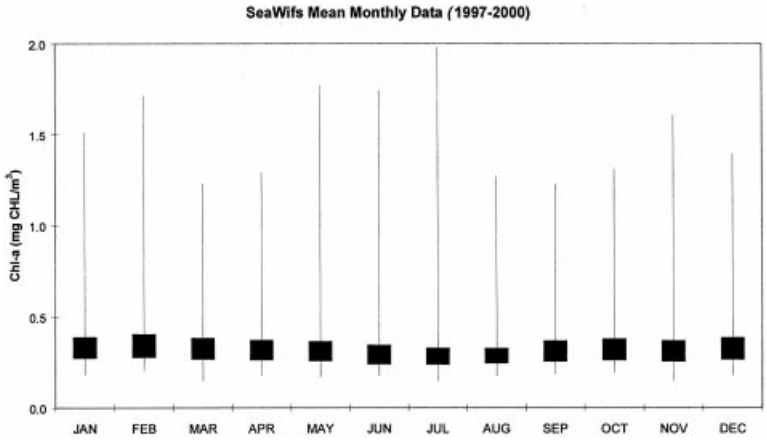

Fig. 3. Satellite-derived, monthly euphotic zone chlorophyll-*a* for the study region (box is mean $\pm$std deviation; whiskers are maximum and minimum values).

The flux is predicted to increase by approximately 5% in this run. The uncertainty analysis resulted in a trend line slope of (0.45 ± 0.32) μmole/m^2/yr and an intercept of (1470 ± 266) μmole/m^2. A negative trend line slope was obtained in less than 2% of the over 300 model runs done in the uncertainty analysis, confirming a positive sign for the ΔF_{DMS}.

The magnitude of the predicted change in DMS flux is similar to our previous findings in G98, which estimated ΔF_{DMS} to be in the range 2% to 8% (Gabric et al., 1998). This was despite a much reduced warming predicted by the coupled GCM compared with the slab-ocean model. However, our previous analysis did not take into account the shoaling of the mixed layer which the coupled GCM predicts will occur during the austral spring (Fig. 2b).

Equilibrium runs. The DMS model did not necessarily achieve equilibrium during any one year of the 120-year transient run. In order to investigate whether this significantly affected our conclusions, a second set of simulations were undertaken with the DMS model run to equilibrium using the decadal average GCM forcings under current and enhanced greenhouse conditions.

The change in the annual cycle in DMS flux is shown in Figs. 6. Under warmed conditions, the DMS production and flux are higher in winter and early spring, presumably due to the earlier shoaling of the mixed layer during this period. The annual integrated flux values for current, doubled and tripled equivalent CO_2 conditions represent a ΔF_{DMS} of about 5% over the 1991–2080 period which is consistent with the results of the transient analysis given above.

5. Conclusions

Coupled atmosphere–ocean GCM simulations of temperature, cloud, wind speed and MLD under enhanced greenhouse conditions have been used to force a regional DMS production model in the Subantarctic Southern Ocean. The GCM simulation was run in transient mode over the time period 1961–2080, and suggested a significant trend in temperature and oceanic mixed layer depth, but no trend in the other meteorological variables. The simulated change in temperature (about 2°K under tripled CO_2 conditions at 2080) was much less than a previous estimate using a "slab-ocean" GCM, which simulated a 4°K rise under doubled CO_2 conditions. The mixed layer depth, which was kept constant in the "slab-ocean" model, was now simulated to undergo a shoaling of about 20% during winter–spring under warmed conditions; however, there was only a slight change simulated in summer-autumn.

Both transient and equilibrium simulations predicted consistent estimates of the effect on DMS flux to the atmosphere, with a mean ΔF_{DMS} of

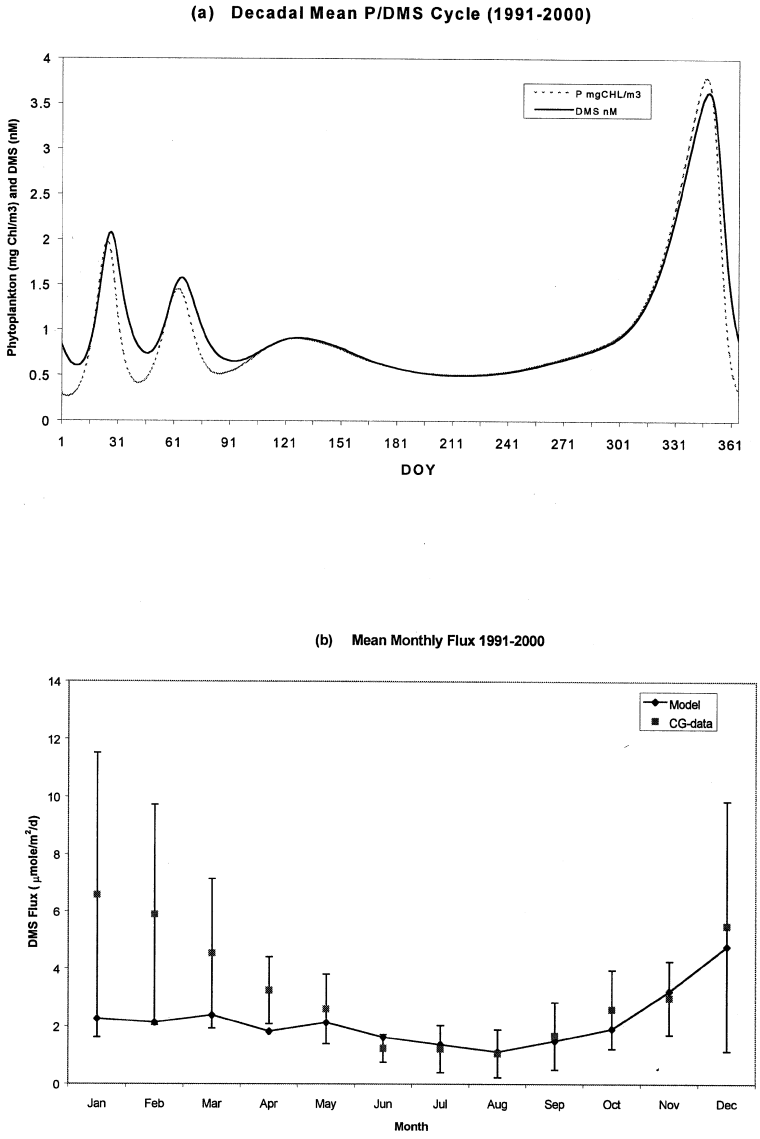

Fig. 4. (a) Predicted annual cycle in mixed layer phytoplankton and DMS, using average forcings for the decade 1991–2000, (b) comparison of predicted flux cycle with Cape Grim data collected over the same period.

+5% by 2080. A Monte-Carlo uncertainty analysis provided a confidence interval on the mean of +1% to +6%. The predicted rate of increase in DMS flux is in a similar range to that estimated previously in G98, however the period for this change to be attained is now longer (2080). Based on the same arguments used in G98, we estimate that the 5% enhanced DMS flux would lead to a $-0.3\ \mathrm{Wm}^{-2}$ radiative forcing (combined direct and indirect). By way of comparison, the CGCM model simulations suggest a tripling of equivalent CO_2 concentration contributes an increase in longwave radiative forcing of the troposphere of $\sim +6.9\ \mathrm{W\,m}^{-2}$ consistent with other climate model simulations (Houghton et al., 1996). The mean DMS flux perturbation thus represents a negative feed-back strength of about 4%.

There are a number of caveats which we should

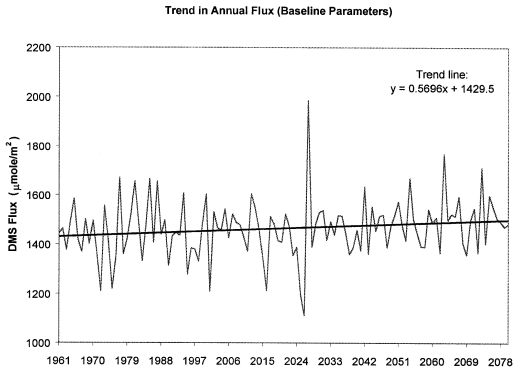

Fig. 5. The trend in annual DMS flux over the 120-year transient simulation.

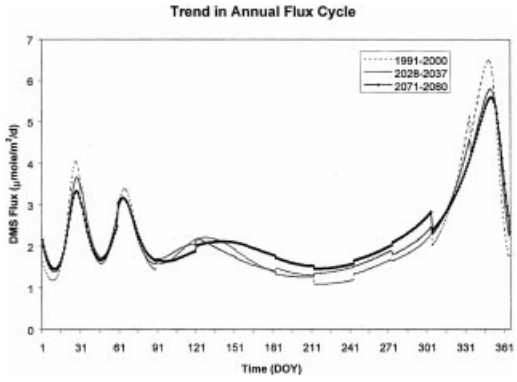

Fig. 6. The annual DMS flux cycle under current, and doubled and tripled CO_2 conditions, relative to pre-industrial levels.

point out. Our study is essentially a regional one and the extrapolation of the results to other parts of the world's oceans should be done with caution. Our analysis was done assuming no significant change in the structure of the marine food-web under warmed conditions. Of particular relevance would be a possible sustained or permanent shift in phytoplankton species composition. It is known that the intracellular concentration of the metabolic precursor of DMS, dimethylsulphoniopropionate, varies between different phytoplankton species over a range of five orders of magnitude (Keller et al., 1989; Liss et al., 1997). Thus, a sustained shift from diatoms to higher DMS producing algal groups such as dinoflagellates and coccolithophores, or vice versa, could have important consequences for the DMS flux trend (Matrai and Keller, 1993).

Strong stratification could be an agent for such a species shift. Although this is not predicted for our particular ocean area, simulations done using the same GCM by Hirst (1999) suggest that strong stratification may indeed occur in the Antarctic Southern Ocean (south of 60°S) by the time of equivalent CO_2 tripling. In addition, stronger warming is simulated at high latitudes (Hirst, 1999) compared with our study region, thus enhanced DMS production is a likely future scenario in the Antarctic ocean, an area where seasonal DMS emissions are already quite high (McTaggart and Burton, 1992). Future computational studies should concentrate on these climatically sensitive polar regions.

Recently, Petchey et al. (1999) reported microcosm experiments where simulated warming altered affected a structural change in the food-web through the removal of the top predators and herbivores. The modified food-web was dominated by autotrophs and bacterivores. If shown to hold generally, this is very important result for both the carbon and sulphur cycles. Zooplankton grazing is thought to be an important mechanism for DMSP and DMS release from algal cells (Dacey and Wakeham, 1986; Leck et al., 1990), and it is the second most influential parameter in our model (Table 5). Experiments conducted by Tang (2000) demonstrated that most of the DMSP ingested by grazers is excreted as faecal pellets and not retained in their body tissues, and that zooplankton may thus also mediate the vertical flux of particulate DMSP in the water column.

Our attempts at simulating the impact of climate change on the DMS cycle are constrained by a lack of information on the ways the food-web might change in a structural sense. To properly assess the impact of warming induced food-web changes on the DMS cycle, it will be necessary to conduct carefully designed ecosystem manipulation experiments where DMS production is monitored. Modellers and empiricists will need to collaborate closely in the future to ensure that the results of such experiments can be applied at regional and ultimately global scales.

6. Acknowledgements

We gratefully acknowledge the financial assistance of an Australian Research Council Large

Grant. The efforts of Martin Dix in furnishing the GCM outputs, and Greg Ayers in supplying the Cape Grim DMS flux estimates are sincerely appreciated. Finally, we are thankful for the detailed comments of two anonymous reviewers which improved the original manuscript significantly.

REFERENCES

Ayers, G. P. and Gras, J. L. 1991. Seasonal relationship between cloud condensation nuclei and aerosol methanosulphonate in marine air. *Nature* **353**, 834–835.

Ayers, G. P., Ivey, J. P. and Gillett, R. W. 1991. Coherence between seasonal cycles of dimethylsulfide, methanesulphonate and sulphate in marine air. *Nature* **349**, 404–406.

Ayers, G.P, Bentley, S. T., Ivey, J. P. and Forgan, B. W. 1995. Dimethylsulphide in marine air at Cape Grim, 41S. *J. Geophys. Res.* **100**, 21013–21021.

Ayers G. P., Cainey J. M., Granek, H. and Leck C. 1996. Dimethylsulfide oxidation and the ratio of methanesulfonate to non sea-salt sulfate in the marine aerosol. *J. Atmos. Chem.* **25**, 307–325.

Baker, K. S. and Frouin, R. 1987. Relation between photosynthetically available radiation and total insolation at the ocean surface under clear skies. *Limnol. Oceanogr.* **32**, 1370–1377.

Bates, T. S., Lamb, B. K., Guenther, A., Dignon, J. and Stoiber, R. E. 1992. Sulfur emissions to the atmosphere from natural sources. *J. Atmos. Chem.* **14**, 315–337.

Berresheim, H., Andreae, M. O., Iverson, R. L. and Li, S. M. 1991. Seasonal variations of dimethylsulfide emissions and atmospheric sulfur and nitrogen species over the western north Atlantic Ocean. *Tellus* **43B**, 353–372.

Boers, R., Ayers, G. P. and Gras, J. L. 1994. Coherence between seasonal variation in satellite-derived cloud optical depth and boundary-layer CCN concentrations at a midlatitude Southern hemisphere station. *Tellus* **B46**, 123–131.

Brock, T. D. 1981. Calculating solar radiation for ecological studies. *Ecol. Model.* **14**, 1–19.

Brutsaert, W. 1982. *Evaporation into the atmosphere: theory, history and applications*. D. Reidel Publishing, Dordrecht, Holland.

Camponlongo, F. and Gabric, A. J. 1996. The parametric sensitivity of the sea-to-air flux of dimethylsulphide in the Southern Ocean. In: *Proc. Symposium on Theory and applications of sensitivity analysis of model output in computer simulation, Belgirate, Sept. 1995* (Saltelli A and von Maravic, H eds). European Commission Rep. EUR 16331, 137–139.

Charlson, R. J, Lovelock, J. E., Andreae, M. O. and Warren, S. G. 1987. Oceanic phytoplankton, atmospheric sulphur, cloud albedo and climate. *Nature* **326**, 655–661.

Clementson, L. A., Parslow, J. S., Griffiths, F. B., Lyne, VD, Mackey, D. J., Harris, G. P., McKenzie, D. C., Bonham, P. I., Rathbone, C. A. and Rintoul, S. 1998. Controls on phytoplankton production in the Australian sector of the subtropical convergence. *Deep Sea Res.* **45**, 1627–1661.

Cox, M. D. 1984. *A primitive equation, 3-dimensional model of the ocean*. GFDL Ocean Group Tech. Rep. No. 1, GFDL/Princeton University, Princeton University, Princeton, N. J. 141pp.

Curran, M. A. J., Jones, G. B. and Burton, H. 1998. Spatial distribution of dimethylsulfide and dimethylsulfoniopropionate in the Australasian sector of the Southern Ocean. *J. Geophys. Res.* **103**, 16,677–16,689.

Dacey, J. W. H. and Wakeham, S. G. 1986. Oceanic dimethylsulfide: production during zooplankton grazing on phytoplankton. *Science* **233**, 1314–1316.

De Bruyn, W. J., Bates, T. S., Cainey, J. M. and Saltzman, E. S. 1998. Shipboard measurements of dimethyl sulfide and SO_2 southwest of Tasmania during the First Aerosol Characterisation Experiment (ACE-1). *J. Geophys. Res.* **103**, 16703–16711.

Eppley, R. W. 1972. Temperature and phytoplankton growth in the sea. *Fish. Bull.* **70**, 1063–1085.

Erickson, D. J., Ghan, S. J. and Penner J. E. 1990. Global ocean-to-atmosphere dimethyl sulfide flux. *J. Geophys. Res.* **95**, 7543–7552.

Foley, J. A., Taylor, K. E. and Ghan, S. J. 1991. Planktonic dimethylsulfide and cloud albedo: an estimate of the feedback response. *Clim. Change* **18**, 1–15.

Gabric, A. J., Murray, C. N., Stone, L. and Kohl, M. 1993. Modelling the production of dimethylsulfide during a phytoplankton bloom. *J. Geophys. Res.* **98**, 22805–22816.

Gabric, A. J., Ayers, G. P. and Sander, G. C. 1995. Independent marine and atmospheric model estimates of the sea-air flux of dimethylsulfide in the Southern Ocean. *Geophys. Res. Lett.* **22**, 3521–3524.

Gabric, A. J., Ayers, G. P., Murray C. N. and Parslow, J. 1996. Use of remote sensing and mathematical modelling to predict the flux of dimethylsulphide to the atmosphere in the Southern Ocean. *Adv. in Space Res.* **18**, 117–128.

Gabric, A. J., Whetton, P., Boers, R. and Ayers, G. P. 1998. The impact of GCM predicted climate change on the air-to-sea flux of dimethylsulphide in the sub-antarctic Southern Ocean. *Tellus* **50B**, 388–399.

Geider, R. J. 1987. Light and temperature dependence of the carbon to chlorophyll *a* ratio in microalgae and cyanobacteria: Implications for physiology and growth of phytoplankton. *New Phyto.* **106**, 1–34.

Gent, P. R. and McWilliams, J. C. 1990. Isopycnal mixing

in ocean circulation models. *J. Phys. Oceanogr.* **20**, 150–155.

Goldman, J. C. and Carpenter, E. L. 1974. A kinetic approach to the effect of temperature on algal growth. *Limnol. Oceanogr.* **19**, 756–766.

Gordon, H. G. and O'Farrell, S. P. 1997. Transient climate change in the CSIRO coupled model with dynamic sea ice. *Mon. Weather Rev.* **125**, 875–907.

Griffiths, F. B., Bates, T. S., Quinn, P. K., Clementson, L. A. and Parslow, J. S. 1999. Oceanographic context of the First Aerosol Characterisation Experiment (ACE 1): A physical, chemical, and biological overview. *J. Geophys. Res.* **104**, 21,649–21,671.

Harris, G. P., Nilsson, C., Clementson, L. A. and Thomas, D. 1987. The water masses of the east coast of Tasmania: Seasonal and internannual variability and the influence on phytoplankton biomass and productivity. *Aust. J. Mar. Freshwater Res.* **38**, 569–590.

Hirst, A. C. 1999. The Southern Ocean response to global warming in the CSIRO coupled ocean–atmosphere model. *Environ. Mod. & Software* **14**, 227–241.

Hirst, A. C., O'Farrell, S. P. and Gordon, H. B., 2000. Comparison of a coupled ocean–atmosphere model with and without oceanic eddy-induced advection. Part I: Ocean spinup and control integrations. *J. Climate* **13**, 139–163.

Houghton, J. T., Meira Filho, L. G., Callander, B. A., Harris, N., Kattenberg, A. and Varney, S. K. (eds.) 1996. *Climate change 1995: contribution of working group I to the second assessment report of the IPCC*. Cambridge University Press, Cambridge, 572 pp.

Jahne B, and Haussecker, H. 1998. Air–water gas transfer. *Ann. Rev. Fluid Mech.* **30**, 443–468.

Jones, G. B., Curran, M. A.J., Swan, H. S., Greene, R. M., Griffiths, F. B. and Clementson, L. A. 1998. Influence of different water masses and biological activity on dimethylsulphide and dimethylsulphoniopropionate in the subantarctic zone of the Southern Ocean during ACE-1. *J. Geophys. Res.* **103**, 16,691–16,701.

Kattenberg, A., Giorgi, F., Grassl, H., Meehl, G. A., Mitchell, F. B., Stouffer, R. J., Tokioka, T., Weaver, A. J. and Wigley, T. M. L. 1996. *Climate models — projections of future climate*. In: *Climate change 1995: the science of climate change*, Houghton, J. T. et al. (eds.). Cambridge University Press, Cambridge, UK, pp. 285–357.

Keller, M. D., Bellows, W. K. and Guillard, R. L. 1989. Dimethyl Sulfide production in marine phytoplankton. In: *Biogenic sulfur in the environment*, Saltzman E. S. and Cooper W. J. (eds.). American Chemical Society, Washington, DC, USA.

Kettle, A. J. et al. 1999. A global database of sea surface dimethylsulfide (DMS) measurements and a procedure to predict sea surface DMS as a function of latitude, longitude and month. *Global Biogeochem. Cycles* **13**, 399–444.

Kieber, D. J., Jiao, J., Kiene, R. P. and Bates, T. S. 1996. Impact of dimethylsulfide photochemistry on methyl sulfur cycling in the equatorial Pacific. *J. Geophys. Res.* **101**, 3715–3722.

Kiene, R. P. 1990. Dimethyl sulfide production from dimethyl sulfoniopropionate in coastal seawater samples and bacterial cultures. *Appl. Environ. Microbiol.* **56**, 3292–3297.

Kiene, R. P., Linn, L. J. and Bruton, J. A. 2000. New and important roles for DMSP in marine microbial communities. *J. Sea Res.* **43**, 209–224.

Kiene, R. P. and Bates, T. S. 1990. Biological removal of dimethylsulfide from seawater. *Nature* **345**, 702–705.

Koga, S. and Tanaka, H. 1993. Numerical study of the oxidation process of dimethylsulphide in the marine atmosphere. *J. Atmos. Chem.* **17**, 203–228.

Lawrence, M. G. 1993. An empirical analysis of the strength of the phytoplankton–dimethylsulfide–cloud–climate feedback cycle. *J. Geophys. Res.* **98**, D11, 20,663–20,673.

Leck, C., Larsson, U., Bgander, L. E., Johansson, S. and Hajdu, S. 1990. DMS in the Baltic Sea — annual variability in relation to biological activity. *J. Geophys. Res.* **95** (C3), 3353–3363.

Levasseur, M., Michaud, S., Egge, J., Cantin, G., Nejstgaard, J. C., Sanders, R., Fernandez, E., Solberg, P. T., Heimdal, B. and Gosselin. 1996. Production of DMSP and DMS during a mesocosm study of an *Emiliana huxleyi* bloom: influence of bacteria and *Calanus finmarchicus* grazing. *Mar. Biol.* **126**, 609–618.

Lewis, M. R. 1995. Coastal zone color scanner on nimbus and sea-viewing wide field-of-view sensor on Seastar. In: *Oceanographic applications of remote sensing*, M. Ikeda and F. W. Dobson (eds). CRC Press, Boca Raton, Florida, pp. 167–181.

Liss, P. S. and Merlivat, L. 1986. Air–sea gas exchange rates: introduction and synthesis. In, *The role of air–sea exchange in geochemical cycling*, P. Buat-Menard (ed). Reidel, Hingham, MA, pp. 113–127.

Liss, P. S., Malin, G., Turner, S. M., Holligan, P. M. 1994. Dimethylsulphide and *Phaeocystis*: a review. *J. Mar. Sys.* **5**, 41–53.

Liss, P. S., Hatton, A. D. Malin, G. Nightingale, P. D. and Turner, S. M. 1997. Marine sulphur emissions, *Phil. Trans. Roy. Soc. London, Series B* **352**, 159–168.

Matrai, P. A. and Keller, M. D. 1993. Dimethylsulfide in a large-scale coccolithophore bloom in the Gulf of Maine. *Contin. Shelf Res.* **13**, 831–843.

McTaggart, A. R. and Burton, H. 1992. Dimethyl sulfide concentrations in the surface waters of the Australian Antarctic and subantarctic oceans during an austral summer. *J. Geophys. Res.* **97** (C9), 14,407–14,412.

Meszaros, E. 1988. On the possible role of the biosphere in the control of atmospheric clouds and precipitation. *Atmos. Environ.* **22**, 423–424.

Morel, A. and Berthon, J.-F. 1989. Surface pigments, algal biomass profiles and potential production of the euphotic layer: Relationships reinvestigated in view of remote sensing applications. *Limnol. Oceanogr.* **34**, 1545–1543.

O'Farrell, S. P. 1997. Sensitivity study of a dynamical

sea ice model. The effect of external stresses and land boundary conditions on ice thickness distribution. *J. Geophys. Res.* **103**, 15,751–15,782.

Petchey, O. L., McPhearson, P. T., Casey, T. M. and Morin, P. J. 1999. Environmental warming alters food-web structure and ecosystem function. *Nature* **402**, 69–72.

Platt, T., Denman, K. L. and Jassby A. D. 1977. Modeling the productivity of phytoplankton. In: *The sea*, vol. 6. E. D. Goldberg (ed.). New York, Wiley, pp. 807–856.

Platt, T., Gallegos, C. L. and Harrison, W. G. 1980. Photo-inhibition of photosynthesis in natural assemblages of marine phytoplankton. *J. Mar. Res.* **38**, 687–701.

Pochop, L. O., Shanklin, M. D. and Horner, D. A. 1968. Sky cover influence on total hemispheric radiation during daylight hours. *J. Appl. Meteorol.* **7**, 484–489.

Raven, J. A. and Richardson, K. 1986. Marine environments. In: Baker, N. R. and Long, S. P. (eds.) *Photosynthesis in contrasting environments*. Elsevier Science Publishers.

Saltzman, E. S., King, D. B., Holmen, K. and Leck, C. 1993. Experimental determination of the diffusion coefficient of dimethylsulfide in water. *J. Geophys. Res.* **98**, 16,481–16,486.

Sarmiento, J. L., Slater, R. D. and Fasham, M. J. R. 1993. A seasonal three-dimensional ecosystem model of nitrogen cycling in the North Atlantic euphotic zone. *Global Biogeochem. Cycles* **7**, 417–450.

Shaw, G. E. 1983. Bio-controlled thermostasis involving the sulfur cycle. *Clim. Change* **5**, 297–303.

Simó, R. and Pedrós-Alió, C. 1999. Role of vertical mixing in controlling the oceanic production of dimethyl sulphide. *Nature* **402**, 396–399.

Smith, E. L. 1936. Photosynthesis in relation to light and carbon dioxide. *Proc. Nat. Acad. Science* (Wash.) **22**, 504–511.

Smith, R. C. 1981. Remote sensing and the depth distribution of ocean chlorophyll. *Mar. Ecol.* **5**, 359–361.

Steele, J. H. 1962. Environmental control of photosynthesis in the sea. *Limnol. Oceanogr.* **7**, 137–150.

Stefels, J. and Van Boekel, W. H. M. 1993. Production of DMS from dissolved DMSP in axenic cultures of the marine phytoplankton species P. pouchetii. *Mar. Ecol. Prog. Ser.* **97**, 11–18.

Talling, J. F. 1957. Photosynthetic characteristics of some freshwater plankton diatoms in relation to underwater radiation. *New Phytol.* **56**, 29–50.

Tang, K. W. 2000. Dynamics of dimethylsulfoniopropionate (DMSP) in a migratory grazer: a laboratory simulation study. *J. Expt. Mar. Biol. Ecol.* **243**, 283–293.

Taylor, B. F. and Gilchrist P. T. 1996. Metabolic pathways involved in DMSP degradation. In: *Biological environmental chemistry of DMSP and related sulfonium compounds*, edited by R. P. Kiene, P. T. Visscher, M. D. Keller, and G. O. Kirst. Plenum Press, New York, pp. 265–276.

Valiela, I. 1995. *Marine ecological processes*, 2nd edition. Springer-Verlag, New York.

Whetton, P., England, M., O'Farrell, S. P., Watterson, I. and Pittock, A. B. 1996. Global comparison of the regional rainfall results of enhanced greenhouse coupled and mixed layer ocean experiments: implications for climate change scenario development. *Climatic Change* **33**, 497–519.

Wilson, S. R. and Ayers, G. P. (eds) 1990. *Baseline atmospheric program (Australia) 1988*. Report produced jointly by Bureau of Meteorology and CSIRO Division of Atmospheric Research, published by Impress Studios, Newcastle, NSW.

Wolfe, G. V. and Kiene R. P. 1993. Radioisotope and chemical inhibitor measurements of dimethyl sulfide consumption rates and kinetics in estuarine waters. *Mar. Ecol. Prog. Ser.* **99**, 261–269.

Wolfe, G. V., Sherr E. B. and Sherr B. F. 1994. Release and consumption of DMSP from *Emiliana huxleyi* during grazing by *Oxyrrhis marina*. *Mar. Ecol. Progr. Ser.* **111**, 111–119.